Philosophical Magazine Part A: Materials Science, Volume 103, Issue 3, 2023, pp. 203-222
DOI:10.1080/14786435.2022.2139421

Insights into the stability of retained austenite during wear

Suruj Protim Neog[1, 2], Arijit Lodh[3], Anish Karmakar[1], Akhil G. Nair[4],Arup Dasgupta[4,]

Subhankar Das Bakshi[5], Sourav Das[1*]

[1] Indian Institute of Technology Roorkee, Roorkee, PIN 247667, India

[2] Indian Institute of Technology Bombay, Powai, PIN 400076, India

[3] Cranfield University, United Kingdom

[4] Indira Gandhi Center for Advanced Research and HBNI, Kalpakkam, PIN: 603102, India

[5] Research and Development Division, Tata Steel Limited, Jamshedpur, PIN 831007, India

*Corresponding author: sourav.das@mt.iitr.ac.in

Abstract

Transformation induced plasticity mechanism is a very interesting phenomenon wherein a certain amount of austenite, which is thermally stable at room temperature but can be transformed to martensite during deformation, is retained in the microstructure. The amount of deformation (either by tensile, compressive or shear) that the austenite regions can withstand before they transform to martensite depends on their stability which is a function of the chemical free energy and the severity of straining. In the current work, a bainitic steel with some retained austenite (RA), exposed to sliding wear in a pin-on-disc wear testing machine, was considered for the study. This paper aims to quantify the shear strain developed in the deformed subsurface region due to wear by using a simple image digitisation technique, and the stability aspect of RA for a complicated deformation mechanism like wear was studied considering the thermodynamics of austenite to ferrite transformations.

Keywords: Wear, subsurface deformation, carbide-free bainite; deformation induced martensitic transformation, model development

Published by Taylor and Francis. This is the Author Accepted Manuscript issued with: Creative Commons Attribution Non-Commercial License (CC:BY:NC 4.0).
The final published version (version of record) is available online at DOI:10.1080/14786435.2022.2139421. Please refer to any applicable publisher terms of use.

Accepted manuscript

Accepted for publication in Philosophical Magazine, DOI:
10.1080/14786435.2022.2139421

1. Introduction

Material damage as a result of wear is a major industrial problem. It causes a considerable expenditure on maintenance and replacement of worn out components[1]. All over the world, substantive efforts are on to mitigate such concerns by developing different steel grades with superior wear resistant properties. Carbide free bainitic steel is one such material[2,3]. It contains a finite volume fraction (~ 15-30%) of retained austenite (RA), which can be transformed to martensite providing a transformation induced plasticity (TRIP) effect, depending on the requirement[2-6]. Several works have been conducted in this direction and many have reported excellent wear resistant behaviour of such steels[2,5,7-9]. It has been postulated that the deformation induced transformation of the retained austenite to martensite is primarily behind such good wear resistant behaviour[3,6,8].

Appreciating the importance of such deformation induced transformation of RA towards achieving the desired mechanical properties, several researchers have worked on understanding such transformation behaviour earlier. The most significant aspects of such quantifications are to determine the temperature at which the RA would start transforming to martensite (*i.e.*, to define the M_s during deformation) and the associated stress/strain level required for such transformation[10-12]. Some early works have tried to thermodynamically define the M_s temperature of such RA islands by combining chemical stability originating due to the compositional difference along with mechanical stability arising from the size effect or extra energy provided by the deformation[13-15]. Some other researchers have concentrated on estimating the deformation condition (in terms of stress or strain), which can trigger such transformation[16-18].

In order to develop the fundamental understanding of deformation induced transformations of RA, researchers have primarily performed uniaxial tensile testing under

Accepted manuscript

Accepted for publication in Philosophical Magazine, DOI:
10.1080/14786435.2022.2139421

various conditions by changing the total strain (ε) or the strain rate (ε') or grain size *etc*[16,19-21]. However, other modes of deformations like shear, fatigue, or compression have rarely been considered in developing these types of models, although those modes of deformations are also quite important from the application point of view[22,23]. It can thus be well appreciated that the deformation behaviour of such RA under complex loadings, such as during shear, which is the prevalent deformation mechanism during wear, can be a vital aspect to study in order to understand its extent of stability fundamentally. Knowledge gained through such development will help in developing newer steel with better resistance to wear by controlling the extent of the transformation of RA.

It was observed in a recent work conducted by Blonde and co-workers[24] that the TRIP effect can be seen during shear deformation upto a wider extent compared to uniaxial loading. In another study by Pyshmintsev et al.[25], hydrostatic pressure was applied during tensile test to change the state of stress. It was found that higher hydrostatic pressure could increase the stability of RA and thus postpone the possible diffusionless transformation to take place. However, the extent of transformation of this RA to martensite with respect to the strain generated during wear has rarely been attempted by either experimental or theoretical treatments. One possible reason for such scarcity in literature reports might be the difficulty in measurement of strain in case of wear unlike tensile testing. A direct measurement using extensometer or video analysis of the surface is not possible during wear because of the nature of the experiment itself. Consequently, a post-mortem analysis, which can reliably calculate the amount of strain, is needed to be carried out for proper quantification. The importance of the current work can be visualised from this aspect.

An approach was taken in the current work considering the free energy of austenite to martensite transformation and the extent of deformation due to wear to estimate the amount of austenite content in response to the strain in the through thickness direction of worn out

Accepted manuscript

Accepted for publication in Philosophical Magazine, DOI:
10.1080/14786435.2022.2139421

samples. Some previously proposed models from the literature, which are merely used for uniaxial tensile loading, have been considered in doing so[16,26]. However, the fitting parameter of the model was calculated for a shear deformation by summing strain using a post processing image digitisation technique and by fitting some previously published phase fraction results under different conditions of stress and strain developed during wear testing. The calculation of shear strain from the deformed microstructural constituents has been reported by researchers for pearlitic rail steel[27-29] as well as for some other ductile materials like Ag, Cu, Al [30,31]. Carlsson et al.[28] adopted a methodology for pearlitic steel to quantify strain by manually rotating a grid across the deformed microstructural constituents. Hughes et al. [31] had applied a different method for a Cu system to trace extended boundaries in Cu from the TEM images to quantify strain. However, in most cases, the strain measurements were carried out very close to the worn surface (within a depth of upto 10 μm only). The novelty of this current work can be found through the correlation of the calculated shear strain with the possible TRIP effect that can predominantly change the rate at which the material is worn out.

However, the depths upto which the effect of deformation actually has reached need to be known before estimating strain. Considering this, it was felt necessary to conduct EBSD measurement in the through thickness direction. Nevertheless, EBSD has the limitation of indexing a highly strained material as well as phase identification in those regions leading to a poorer extent of indexing with increasing deformation[32,33]. Consequently, the depth at which EBSD indexing of the worn sample would match with the indexing of the undeformed sample was considered the minimum depth upto which the deformation could affect the microstructure. For this reason, the phase fraction result of RA using EBSD was not considered for quantitative purposes although knowing the amount of RA is a critical requirement. Alternatively, the phase fraction of RA was estimated using the analysis of XRD data. The challenge was to perform the XRD experiments at a sequential distance from the worn surface.

Accepted manuscript

Accepted for publication in Philosophical Magazine, DOI:
10.1080/14786435.2022.2139421

Therefore, XRD acquisitions were carried out at known depths from the surface by mechanically removing material to desired depths from the surface. EBSD was thus only used as a guiding tool rather than either a phase or strain quantification technique in this work.

Finally, the predictions of the model were compared with the sequential XRD measurements at various depths. The model predictions of the amount of RA turned out to be within a fair degree of approximation with the experimental estimations. It is thus expected that the model can be utilised for estimating the evolution of martensite during wear study for other steel grades as well because of the generic nature of the parameters.

2. Experimental procedure

A carbide free bainitic (CFB) steel with 0.34% C, 1.50% Si, 1.80% Mn, and 0.93% Cr (all in wt%) and other alloying elements in unavoidable amount was considered for this present investigation. The as-received microstructure at room temperature comprises ~75% bainitic ferrite, ~20% RA, and ~5% martensite with ~1370 MPa ultimate tensile stress and ~21% total elongation[34-38]. The steel was hot rolled upto 3 mm thickness with a finish rolling temperature of 880 ^{o}C (in fully austenitic condition), rapidly cooled upto above bainite start temperature, and coiled and left for natural cooling.

Cylindrical samples with a diameter of 6 mm and thickness of 3 mm were cut out of the hot-rolled sheets to expose them to wear testing in a pin on disc tribometer, which is essentially a shear deformation mechanism. ASTM G99 standard procedure was followed during the operation [39]. The schematic representation of the testing rig and methodology used to obtain different samples for characterisations are shown in Fig. 1. Dry sliding wear tests were performed in a controlled laboratory environment with 27± 3 ^{o}C temperature and relative humidity was within 45± 5 %. EN31 bearing steel disc having hardness about 730± 10 HV was used as a counterface material against the cylindrical pin samples and tests were

Accepted manuscript

Accepted for publication in Philosophical Magazine, DOI:
10.1080/14786435.2022.2139421

performed under varying conditions of load (10 to 50 N), and distance slid (7.2 km and 18 km). A sliding speed of 1 m/s was maintained at the contact point of the pin and the disc. Pin samples and the disc were grounded and appropriately cleaned before individual tests. The weight losses of both the pin and the disc were recorded with a precision balancing machine having readability up to 0.1 mg as a measurement of the wear resistance under varying conditions of load and distance slid.

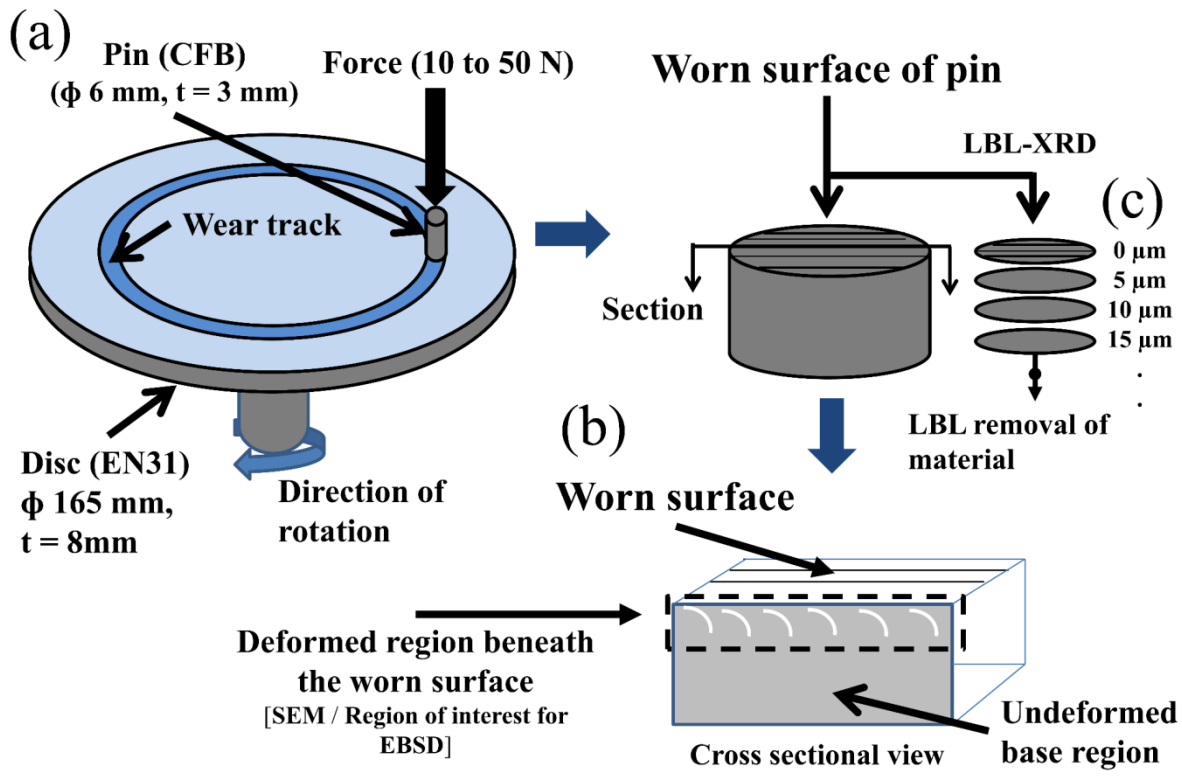


Fig. 1. Schematic diagrams of (a) pin on disc wear testing setup, (b) region for EBSD, (c) controlled and sequential removal of material.

After the wear test, a meticulous procedure was followed to extract information regarding the presence of retained austenite in the sub-surface region of the worn samples by XRD. Two representative samples were chosen for such successive removal of material of specific thickness from the top surface of the sample. The precise layer by layer (LBL) removal of the material was performed using a Gatan disc grinder. The process uses negligible pressure

Accepted for publication in Philosophical Magazine, DOI:
10.1080/14786435.2022.2139421

during the grinding operation, ensuring minor chances of material damage that could trigger any transformations of RA to martensite during the process itself. It is to mention here that the same equipment is very frequently used for preparing TEM samples as well, where the introduction of minute stress during sample preparation is not accepted[40,41]. XRD experiments were conducted on the freshly opened surface after the precise removal of every layer. Fig. 1c schematically describes such an experimental scheme. In order to minimise the depth of penetration and restrict obtaining the information from a deeper region, a Cu target was used with 0.015° per step and 5 seconds for each step, covering a 2-theta range of 40°-125° using Brag-Brentano parafocussing geometry.

A few specimens from the cross-sectional area of wear samples (see Fig. 1b) were prepared by conventional metallography and electropolishing (electrolytic solution of acetic acid and methanol with 1:9 ratio, 10 V for 20 seconds at 283K) to characterise using EBSD for estimating the depth upto which wear experiments made a significant and noticeable impression in the subsurface regions. Zeiss-Sigma-300 Field Emission Scanning Electron Microscope (FE-SEM) at 20 kV equipped with Oxford Instruments C-Swift EBSD detector and TSL-OIM^{TM} software was used for crystal orientation data measurement and post-processing/analysis. The scans were performed using a step size of 0.1 µm over an area of 81 x 108 µm^2. Three separate regions were scanned for each sample to ensure data reproducibility. The working distance was kept as 10 mm, and all camera/scan settings were kept identical between the scans for proper comparison. FCC austenite and BCC ferrite were chosen from the EBSD database as the phases. The sole objective of using EBSD in this operation was to visualise the extent of deformation in order to guide the strain calculation using image analysis and material removal during the LBL-XRD experiment.

3. Model development

Accepted manuscript

Accepted for publication in Philosophical Magazine, DOI:
10.1080/14786435.2022.2139421

An effort was put into developing an empirical model to predict the extent of deformation induced transformation of metastable austenite, as no model currently exists that can define the stability of austenite under the influence of wear to the best of the knowledge of the authors. Sugimoto *et al.* [16] had proposed a model earlier for predicting the stability of RA for tensile deformation. According to that theory, if V_γ^O is the volume fraction of RA at a zero strain ($\varepsilon = 0$) and V_γ is the fraction left untransformed at a particular strain ε, they can be correlated as:

$$\frac{V_\gamma^0}{V_\gamma} = e^{k\varepsilon} \quad (1)$$

where k is a fitting constant determined by plotting the experimental data. After simplifying, Eq1 can be re-written as:

$$\ln(V_\gamma^0) - \ln(V_\gamma) = k.\varepsilon \quad (2)$$

However, it is to be noted here that the effect of compositional differences on the stability aspect of RA and thereby the extent of formation of martensite was not taken into account in this expression. It is worth mentioning that the stability of austenite would become higher if it is enriched with elements that are considered austenite stabiliser (*e.g.* C, Mn, Ni *etc.*). In such instances, it would not readily transform to martensite during deformation. How readily the austenite would tend to transform to its product (martensite) would thus depend to a great extent on the change in the chemical free energy ($\Delta G^{\gamma\rightarrow\alpha'} = \Delta G^{\alpha'} - \Delta G^{\gamma}$) of the final system at the temperature and of course on the severity of deformation (ε). A lower value of $\Delta G^{\gamma\rightarrow\alpha'}$ would indicate that the system favours the formation of martensite over austenite and thus the formation of martensite would be facilitated. It is therefore logical to assume that this free energy change should be accommodated in Eq2 above. One of the simplest ways to express Eq2 in the new form, including the change in chemical free energy term, can be seen below in

Accepted manuscript

Accepted for publication in Philosophical Magazine, DOI:
10.1080/14786435.2022.2139421

Eq3. It is worth mentioning here that Sheriff *et al.* [26] [26] also proposed a similar form but for a different work subjected to uniaxial tensile loading.

$$\ln\left(V_\gamma^0\right) - \ln\left(V_\gamma\right) = \Delta G^{\gamma\to\alpha'}.k.\varepsilon \quad (3)$$

It is required to know the austenite composition at an analogous temperature to calculate the free energy change ($\Delta G^{\gamma\to\alpha'}$). It has been mentioned earlier that the microstructural constituents of the current steel are 20% retained austenite and 75% bainite, which forms from the parent austenite under paraequilibrium condition. It implies that there would be no change in the concentration of substitutional alloying elements from the bulk composition, but only the concentration of carbon in austenite would be changed as the result of the bainitic transformation. The concentration of carbon in RA was calculated from its lattice parameter values obtained from X-ray diffraction results of the as received sample without being exposed to wear and subsequently by using the relationship proposed by Dyson and Holmes[42]. It was found that the RA of this material under consideration had a C content of approximately 1.08 wt.% [35,36]. Consequently, as shown in Fig. 2, the free energy calculations were carried out using TCFE7 database available in ThermoCalc software considering the composition as discussed above[43]. The free energy difference between the two phases FCC and BCC was calculated to be -2241 J/mol at a room temperature condition of 298 K.

Accepted manuscript

Accepted for publication in Philosophical Magazine, DOI:
10.1080/14786435.2022.2139421

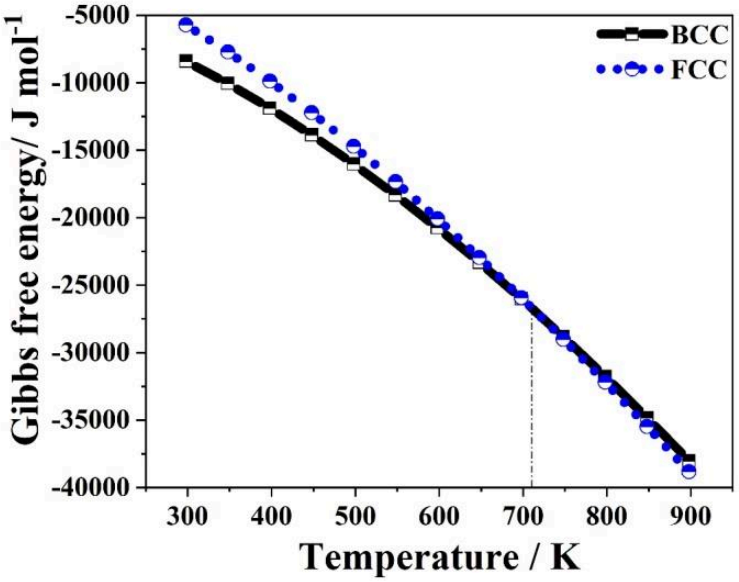


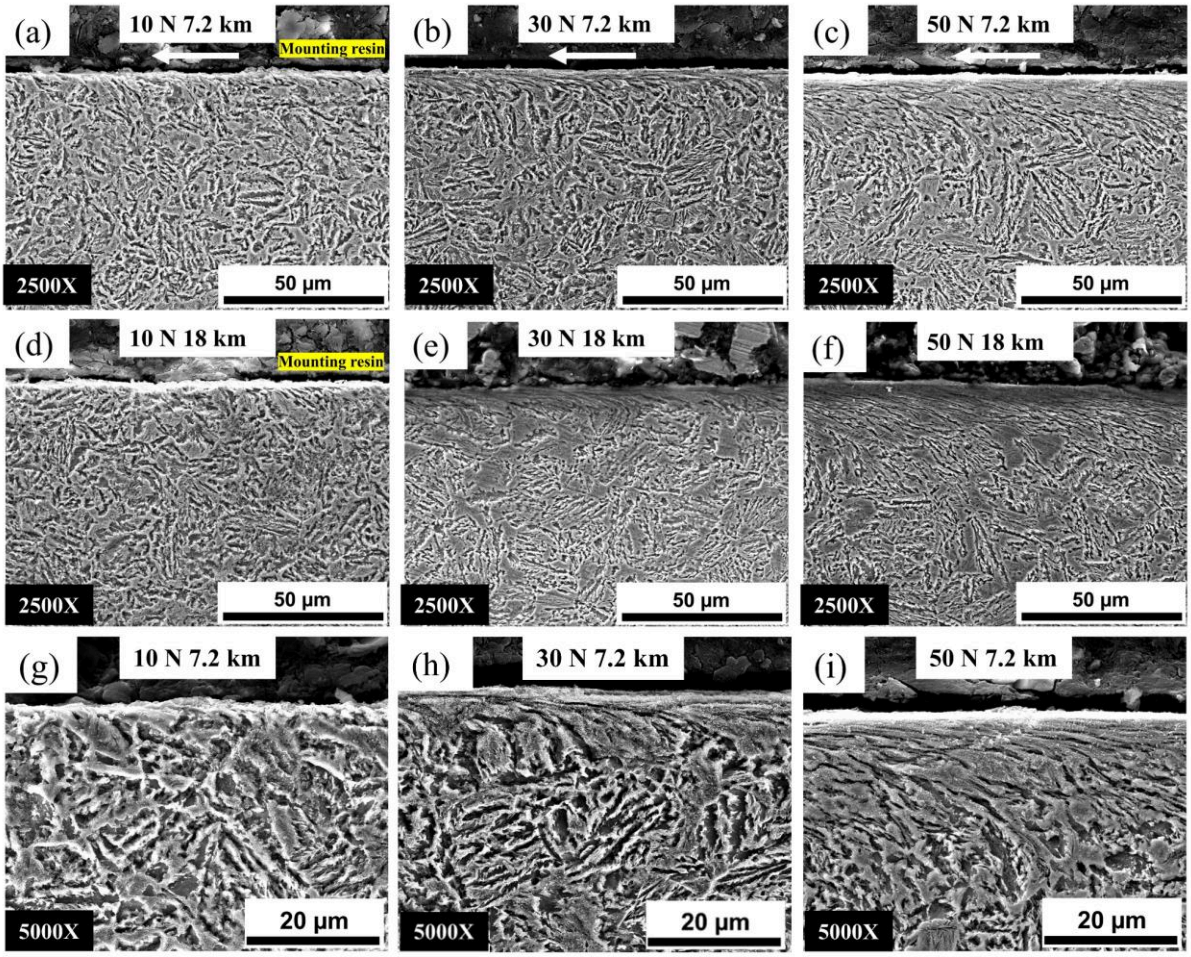
Fig. 2. Showing free energy difference between the FCC and BCC phase as a function of temperature

No direct assessment of strain (ε) was possible due to the nature of wear related experiments. During wear, the extent of deformation decreases towards the deeper inside the material, which is away from the surface. Such a feature can be best observed in the cross sectional images of samples. The formation of bend microstructural feature and corresponding shear strain at the cross section of samples subjected to sliding or rolling/sliding wear can be considered as a very generic and had been proposed by many earlier researchers[7,44,45]. However, a proper correlation between the degree of bending (or shear strain) and related TRIP effect for metastable microstructure like RA + bainite is very rare to the best of the knowledge of the current authors. The extent of deformation, causing the degree of such bending along the direction of sliding, is the primary reason for the transformation of RA to martensite. It is thus logical to assume that the bending (or the shear strain indeed) is related to the deformation induced transformation of retained austenite in some way.

Accepted manuscript

Accepted for publication in Philosophical Magazine, DOI:
10.1080/14786435.2022.2139421

Neog *et al.* had earlier shown such characteristics for two different sliding distances (7.2 and 18 km) for different loadings [(10, 20, 30, 40, and 50 N)[7,44]. Representative through thickness SEM images of only six samples (10, 30, and 50 N loading; 7.2 and 18 km) out of the total ten samples of the previous studies are shown in Fig. 3 for ready reference. Magnified images for all the three conditions of 7.2 km have been shown in Fig. 3(g-i) for better readability of the deformed subsurface regions. In these images, the upper parts indicate the top surface exposed to wear and the lower parts are the bulk material, away from the worn out surface. Bending of the microstructural constituents at the upper parts (*i.e.* closer to the wear surface) of all the six images is clearly visible. It can also be seen that the extent of such bending increases with the increasing severity of the wear condition. The extent of bending is continuously reduced in the lower parts of the samples away from the abrading surface.

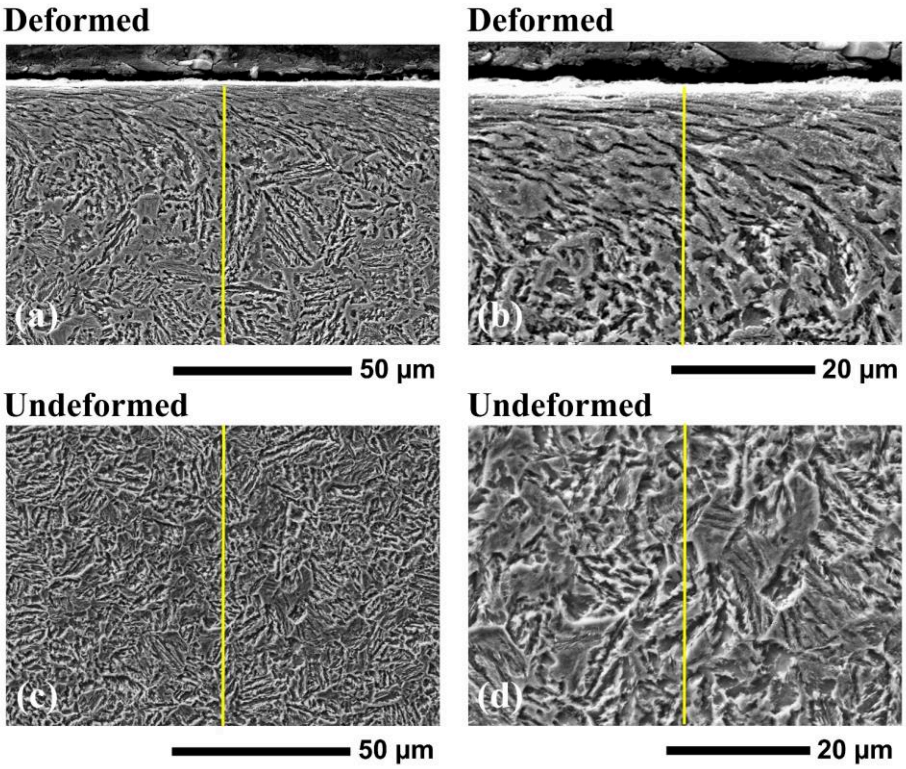


Accepted manuscript

Accepted for publication in Philosophical Magazine, DOI:
10.1080/14786435.2022.2139421

Fig. 3. Microstructure of deformed subsurfaces (a-c) 10-50 N, 7.2 km and 2500X (d-f) 10-50 N, 18 km, and 2500X (g-i) 10-50 N, 7.2 km, and 5000X

The situation can better be appreciated if the cross sectional images of the deformed and the undeformed samples are seen together. In the following image, Fig. 4a and b represent the microstructures of the cross-section of the sample exposed to wear, whereas figures c and d show the microstructures in the through thickness direction of the as-received and undeformed sample. It is to be noted that a and c represent a lower magnification, whereas Fig. 4(b&d) represent a higher one. Random orientation with respect to the vertical line can be seen in Fig. 4c as well as in the lower part of Fig. 4a. Similar observation can also be made for Fig. 4d, which is a much higher magnified image. However, the orientation changes when the microstructure of the region close to the surface, where actual deformation had taken place, is observed (Fig. 4b). A clear indication of the preferred orientation of the microstructure towards the direction of movement can also be seen (Fig. 4b). It can also be noted from Fig. 4c that the microstructures became almost flat and horizontal at very close proximity to the surface.



Accepted for publication in Philosophical Magazine, DOI:
10.1080/14786435.2022.2139421

Fig. 4 Microstructures of the cross section of samples for demonstrating the bending due to wear: a and b. exposed to wear, c and d. undeformed, as-received sample

It can thus be well understood that microstructure get oriented along the direction of wear and a systematic analysis can be developed to quantify the strain the microstructures have experienced during such alignment. Accordingly, a methodology has been adopted in the current work to evaluate the magnitude of shear strain as a function of distance from the worn surface and is shown in Fig. 5a, which is a schematic representation of the bending of the microstructural features. Let us consider the right-angle triangle ABC (ΔABC), of which the right angle is CBA ($\angle CBA$), and the angle 'θ' ($\angle CAB$ in the right angle ΔCAB) is the angle that the deformed microstructural constituent at any point 'O' have made with the normal to the worn surface at a depth of 'y' from the worn surface. The diagram is so drawn that the $\angle CAB$ essentially forms the tangent to the curved line. From the value of 'θ,' the shear strain and the corresponding equivalent strain can be calculated using equations 4-5 shown below[46,47]. Repeating the same procedure over the entire length of the curved line would then provide the extent of the shear strain being experienced by each point. A representative of such an exercise is shown in Fig. 5b, where the trace lines in yellow colour and the triangle have been superimposed on the actual microstructural image for ready comparison. Cross sectional SEM images have been digitised, and the bending of microstructural features have been traced following the procedure as shown in the schematic in Fig. 5a. Strain calculations were carried out at least for ten such separate trace lines for each wear condition to obtain a statistically significant output.

shear strain = $tan\theta$ and (4)

equivalent strain = $\frac{\tan\theta}{\sqrt{3}}$ (5)

Accepted manuscript

Accepted for publication in Philosophical Magazine, DOI:
10.1080/14786435.2022.2139421

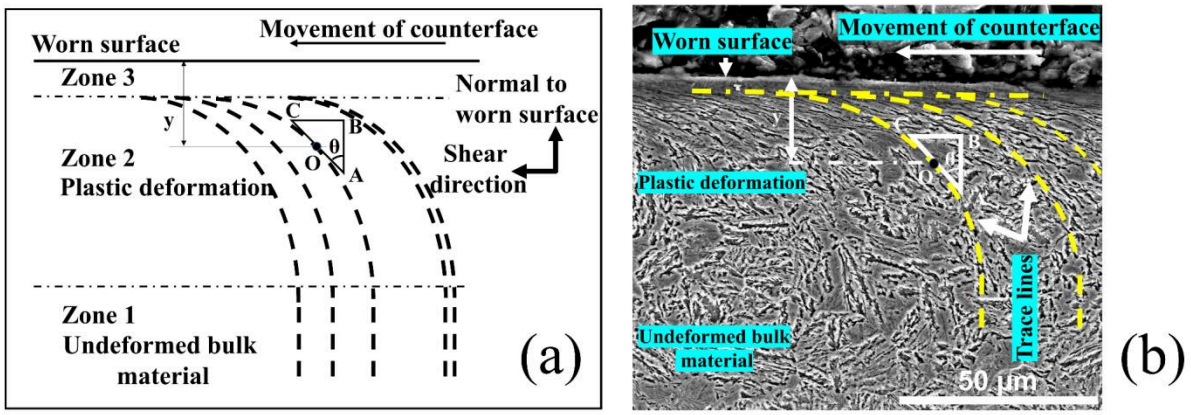


Fig. 5(a) Schematic of deformed tribologically transformed region (Zone 1: Undeformed bulk material, Zone 2: Plastically deformed region, Zone 3: Severely deformed regions with parallel arrangement of microstructural constituents) [7], (b) Methodology to evaluate shear strain by digitising bend grains

The EBSD analysis in the through thickness direction served here as a guiding tool to decide upto how far from the surface layer should such analysis be conducted. The EBSD phase maps for four samples are shown in Fig. 6. It is worth mentioning that no data cleaning procedure was performed during the analysis. Consequently, no force-feeding of the phases was done, and the EBSD software has assigned the BCC and FCC regions for which it was absolutely certain. Thus the final microstructure contains the regions of BCC and FCC along with several locations which were not properly indexed and can be seen in black colours. Such unindexed regions can be developed from the inability of the EBSD software to properly indexing the patterns distorted due to the strain generated during severe plastic deformation or even for the formation of martensitic phase during shear transformation[48,49]. It is logical to consider that the extent of such unindexed regions would be increased with the amount of deformation. Thus any relative change in the unindexed regions from that of the as-received sample may be attributed to the extent of deformation generated during wear testing.

Accepted manuscript

Accepted for publication in Philosophical Magazine, DOI:
10.1080/14786435.2022.2139421

It can be found from Fig. 6 that the unindexed regions, although very small in percentage-wise, are visible for the as-received sample as well. It is because of the presence of high dislocation density generated during bainitic transformation during the formation of microstructure as well as for the presence of martensite in the as-received material. However, such unindexed regions are distributed homogeneously throughout the entire frame indicating the degree of development of strain or the distribution of martensitic regions are almost uniform. This is expected as the development of the microstructure in the as-received material was completely random and never facilitated by any other phenomena. On the contrary, it can be observed from Fig. 6(b, c, d and e) that the extent of unindexed regions for the deformed samples are decreasing from right to left, *i.e.* from surface to the deeper inside the material, and essentially becomes similar to the unindexed regions of the as-received sample at around 50 micron distance from the surface. Thus the extent of unindexed regions can be considered an indirect evidence to understand the depth or distance from the surface upto which the deformation during wear might have any meaningful influence. This indicates that the extent of deformation is decreased from the top surface to the deeper inside the material and at about 50 microns from the surface region, the amount of such deformation can be considered negligible as the level of unindexed areas becomes essentially similar to the as-received sample where no such external deformation was provided.

Accepted manuscript

Accepted for publication in Philosophical Magazine, DOI:
10.1080/14786435.2022.2139421

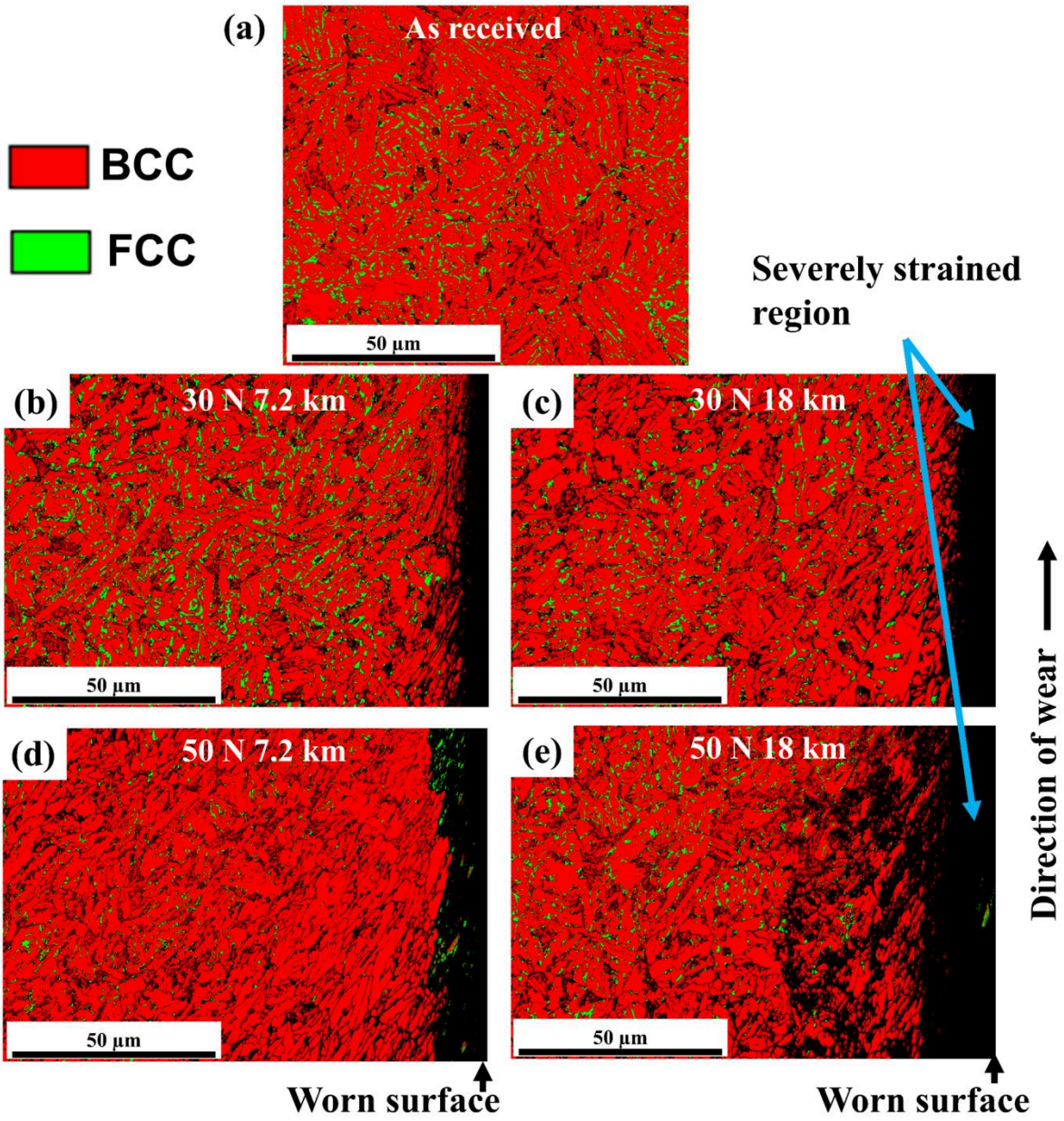


Fig. 6. EBSD phase map of different samples (a) as-received, (b) 30 N 7.2 km, (c) 30 N 18 km, (d) 50 N 7.2 km and (e) 50 N 18 km

Accordingly, the strain was calculated upto 50 micron distance from the surface following the procedure outlined in Fig. 5a, and b. The calculated distribution of equivalent plastic strain (ε) in line with the distance from the worn surface is presented in Fig 7. However, the results of only six samples are shown here to improve the readability. The nature of the curves is quite logical and in accordance with the existing knowledge that the extent of strain

Accepted for publication in Philosophical Magazine, DOI:
10.1080/14786435.2022.2139421

is reduced continuously from the top surface layer to the inside of the material. However, it is worth mentioning here that no shear strain calculation could have been performed for the heavily deformed Zone 3, where microstructural constituents are nearly parallel to the sliding direction ($\theta = 90°$). Accordingly, the regions are kept blank, and no results have been shown.

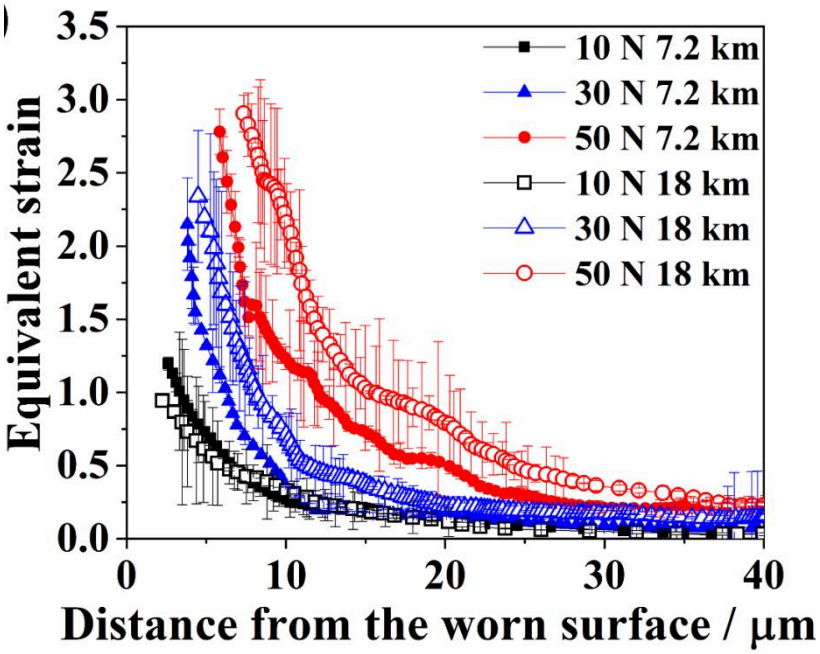


Fig. 7. Equivalent strain as a function of distance

It can thus be appreciated that the primary unknown parameters of the Eq 3, *i.e.* the free energy ($\Delta G^{\gamma\rightarrow\alpha'}$) and the strain ($\varepsilon$), have been successfully resolved, and the only remaining unknown is the value of k, which is a fitting constant. Neog *et al.* had earlier conducted XRD measurements and accordingly have reported the amount of retained austenite present on the top surface, which was exposed to different extent of wear for all the ten conditions (five different loads and two different sliding distances)[7,44]. In developing the model, all these ten samples were utilised for calculating the strain using the image analysis process described above. It is worth mentioning here that the highest strain value that could have been calculated was considered the cause of reduced RA content at the top worn surface. In Table 1, the strain

Accepted Manuscript

Accepted for publication in Philosophical Magazine, DOI:
10.1080/14786435.2022.2139421

and the corresponding V_γ values with their sliding wear conditions are summarized for ready reference. The value of k was calculated for ten different conditions of wear and their average value was considered for further calculations. It can be seen that the value of k was set as (1.7 ± 0.1)×10^{-4} mol $J^{-1,}$ and finally this value only was considered for calculating the retained austenite quantity across the through thickness direction using Eq3.

Table 1: Strain and phase fraction data of austenite to calculate the value of k

Distance / km	**Load / N**	**Strain**	V_γ^0 **% (XRD)**	V_γ **% (XRD)**	k **/ 10^{-4} mol J^{-1}**	**Average k / 10^{-4} mol J^{-}**	**Calculated V_γ % based on average k**
7.2	10	1.19	20.9	13 ± 1	1.7	1.7 ± 0.1	13 ± 1
	20	1.21	20.9	13 ± 1	1.8		13 ± 1
	30	2.15	20.9	10 ± 1	1.6		9 ± 1
	40	2.55	20.9	8 ± 2	1.6		8 ± 1
	50	2.78	20.9	7 ± 2	1.6		7 ± 1
18	10	0.94	20.9	15 ± 2	1.6		15 ± 2
	20	1.41	20.9	14 ± 1	1.3		12 ± 1
	30	2.33	20.9	9 ± 2	1.6		9 ± 1
	40	2.82	20.9	6 ± 1	2.0		7 ± 1
	50	2.9	20.9	6 ± 2	2.0		7 ± 1

This particular value of k for a shear type of deformation is much lower than the already published values for materials subjected to uniaxial tensile deformation[16,19,26,50]. For example, Sherif *et al.*[26] approximated the value of k under uniaxial loadiding as 0.002017

Accepted manuscript

Accepted for publication in Philosophical Magazine, DOI:
10.1080/14786435.2022.2139421

mol Jule^{-1}. This is also logical due to the fact that the magnitude of shear strain could be as high as 2-3, which is practically impossible during tensile deformation, yet the presence of RA is evidenced. Thus obtaining a lower value of k is not something that can't be expected. It is worth mentioning here that the earlier researchers also had observed differences in the value of *k* depending on several parameters like composition, especially the carbon enrichment of the retained austenite or state of stress, *etc.*[19,26]. For example, the transformation of retained austenite under hydrostatic compression would not facilitate the formation of martensite which increases the total volume of the system and thereby has the potential to increase the stability of austenite[25,51,52]. It is thus no wonder to observe a lower *k* value in this current work for transformation under sliding wear. A smaller value of *k* can thus be considered as an indication of greater stability of RA against any deformation induced transformation[16]. This is again in line with the observation of other researchers that austenite is more stable during wear than for uniaxial loading[7,24].

Once the value of the fitting parameter *k* was determined, the model was ready to be used for calculating the amount of RA for the through thickness direction where it was expected that the deformation induced transformation of austenite would occur under the influence of accumulated strain during wear.

5. Comparison with experiment

To validate the model's prediction, XRD was performed on two samples after wear in a layer by layer (LBL) method in the through thickness direction. The result of the EBSD analysis helped in performing this experiment as well. It was considered that the effect of deformation by wear is limited upto a depth of 50 micron from the surface. Accordingly, the XRD patterns were recorded every 5 microns upto 50-micron depth from the surface in order

Accepted manuscript

Accepted for publication in Philosophical Magazine, DOI:
10.1080/14786435.2022.2139421

to quantify the possible change in the microstructural constituents within a shorter region, and after that at every 10-micron interval upto 90 micron depth.

The XRD profiles of the surface of the 30 N 7.2 km sample, after systematic and sequential removal of each layer having the desired thickness are shown in Fig. 8. The LBL-XRD profiles of the other sample subjected to 50 N 7.2 km wear condition was not shown to increase the readability. It suffices to mention here that essentially the similar pattern was also observed for this condition as well. Different crystallographic planes of the bcc bainitic ferrite (α) and fcc retained austenite (γ) are marked in the figure for easy reference. It can be seen from the visual observations that the peak intensities of different austenite planes (111, 200, 220, 311) are increasing as the distance from the worn surface is increasing. This indicates that different amounts of phase fractions of austenite and martensite are present at varying depths from the worn surface to the interior. However, to evaluate the exact amount of different phases present as a function of depth from the worn surface, the full profile fitting Rietveld refinement was performed for all the XRD profiles of the two samples. This is to be noted that suitable .cif (crystallographic information file) files of different phases of steel were used for the Rietveld refinement procedure. The quantified phase fraction results of different XRD profiles were also shown in the next section for better comparisons with the calculated results.

Accepted manuscript

Accepted for publication in Philosophical Magazine, DOI:
10.1080/14786435.2022.2139421

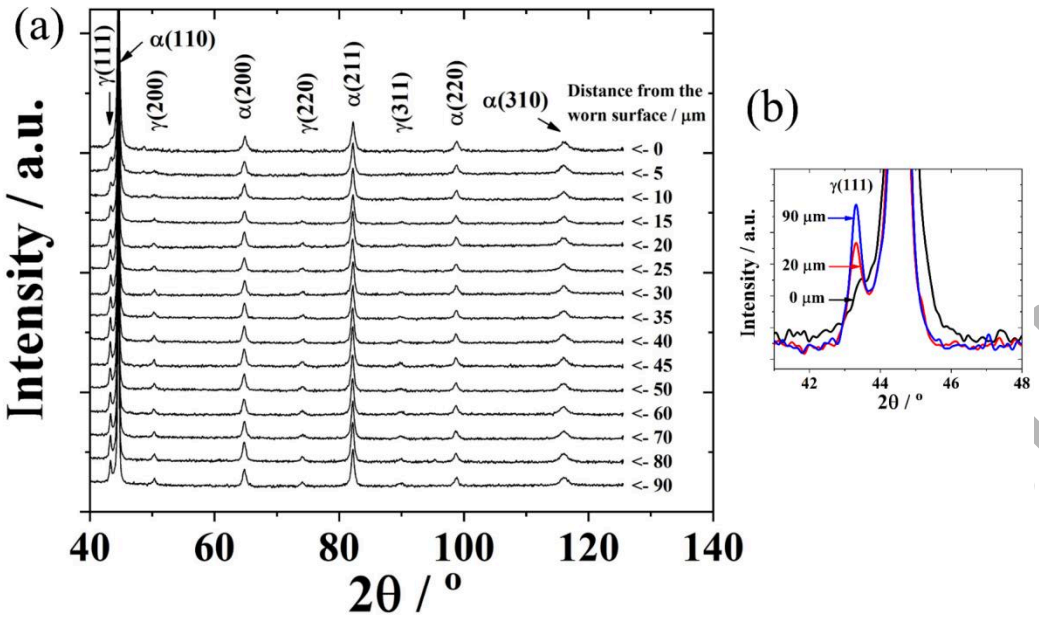


Fig. 8. XRD profiles of sample subjected to 30 N 7.2 km wear condition, (a) different layers of the sample (b) enlarged view of γ (111) plane for 0 μm, 20 μm and 90 μm depth layers.

The model developed above was utilised for calculating the extent of transformation of austenite to martensite under the influence of strain in the through thickness direction. Earlier in Fig. 7, the equivalent strain was plotted against the distance from the worn surface. The amount of RA was calculated following the procedure described above, considering the strain value, and has been plotted in Fig. 9(a) for four different wear conditions. It can be observed from this image that the calculated amount of RA continuously increases with the increase in distance from the worn surface. This signifies that the severe deformation caused by the wear can transform austenite to α'; as this severity is lowered with the increased distance from the worn surface, i.e., towards bulk of the material, higher and higher amount of RA is available there. In Fig. 9(b), the amount of austenite phase is shown as a function of the equivalent strain. The trend is quite expected that the RA diminishes while the strain is increased. It will thus be an interesting one to compare the model predicted and experimentally obtained quantities of RA. The results obtained from the LBL-XRD phase fraction analysis of different samples are shown in Fig. 9(a & b) as a function of distance from the surface and equivalent strain,

Accepted manuscript

Accepted for publication in Philosophical Magazine, DOI:
10.1080/14786435.2022.2139421

respectively. It can be observed that the austenite phase fraction, as calculated from the analytical model and the LBL-XRD of the samples, showed a very close approximation with the strain also. It may be noticed that the austenite phase fraction was decreasing as the strain was increasing. As can be seen in Fig. 9c, the comparison between the calculated and the experimental points showed that the model is showing a slightly higher volume fraction of RA than the experimentally obtained values very near to the worn surface where the amount of RA is very low. The differences between the calculated and the LBL-XRD results may originate from several reasons which include the averaging of the fitting parameter (k) or uncertainities in selecting the highest strain near the edge of the sample due to the presence of white etching layer type features or calculation of free energy at room temperature instead of the actual temperature which might have reached during wear testing due to friction *etc*. However, inspite of these, very good approximation of the model is worth mentioning considering the complexities of the experimental condition.

Accepted manuscript

Accepted for publication in Philosophical Magazine, DOI:
10.1080/14786435.2022.2139421

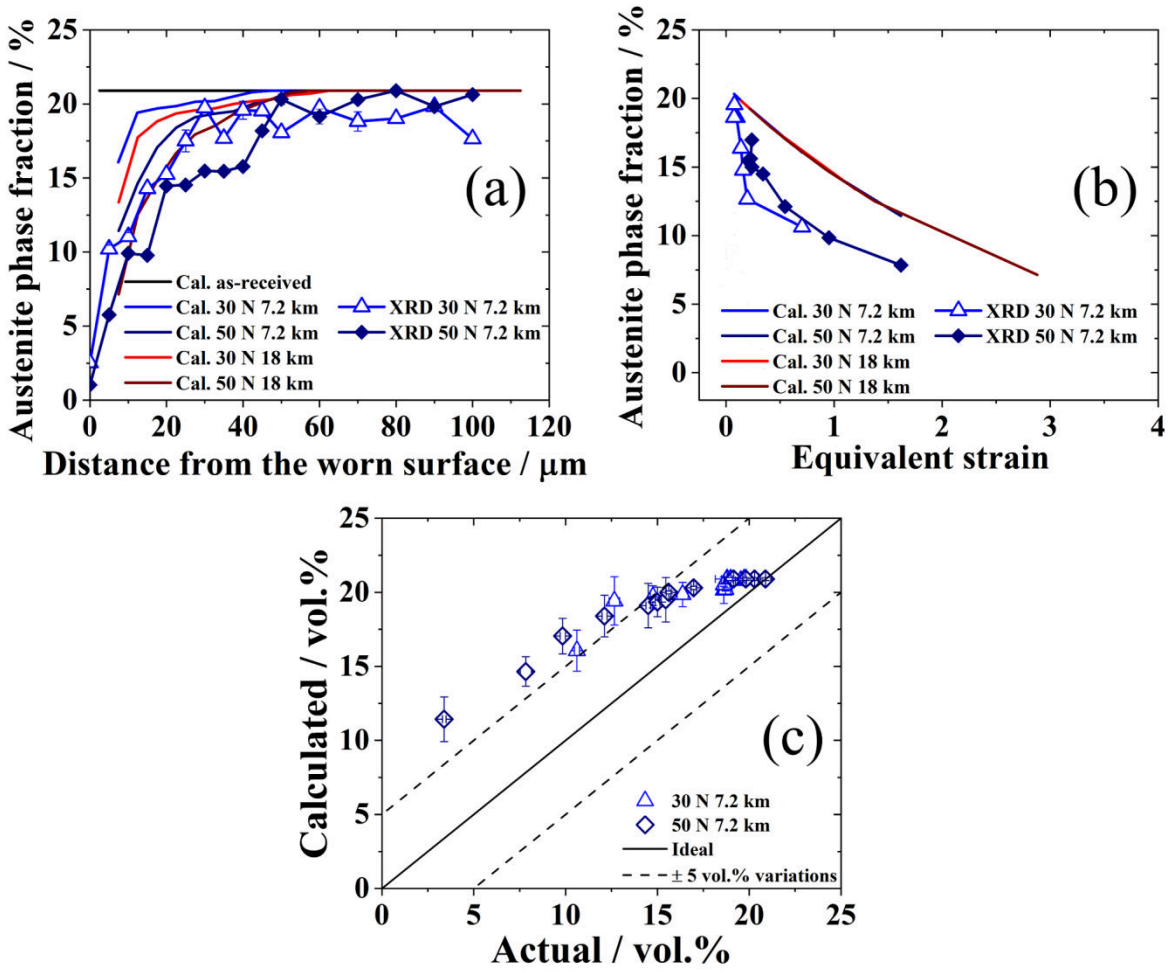


Fig. 9. Comparison of calculated and experimental results obtained from LBL XRD analysis (a) as a function of distance (b) as a function of strain, and (c) degree of agreement between calculated and actual results.

6. Conclusions

In the current work, primarily the evolution of microstructural development (quantification of different phases) in the through thickness direction as well as the stability of retained austenite of a carbide free bainitic steel having metastable austenite and showing transformation induced plasticity during sliding wear under different loading condition was discussed. The key conclusions from the current work can be summarised as follows:

Accepted Manuscript

I. A model has been developed in the current work to predict the amount of untransformed austenite after the application of a certain extent of deformation through wear testing.

II. Calculated results of untransformed austenite in the subsurface regions having exposed to different extent of deformation were compared with the experimental results obtained from layer by layer XRD of the samples.

III. The fair degree of matching between the theoretical prediction of the austenite content with the experimental observation can lead to the development of fundamental understanding of the stability of retained austenite in TRIP aided steel during wear deformation.

IV. This knowledge can further be utilised in developing more accurate models in tailoring the stability of retained austenite for different deformation situation through which novel steel can be designed for wear resistance as well as for other critical applications where the TRIP mechanism can be of significant importance.

Acknowledgement:

A part of this work is partially funded through the grant number: EMR/2017/003627 of Science and Engineering Research Board, Ministry of Science and Technology, Government of India, awarded to SD.

References

[1] K. Holmberg, A. Erdemir, Influence of tribology on global energy consumption, costs and emissions, Friction. 5 (2017) 263–284. https://doi.org/10.1007/s40544-017-0183-5.

[2] S. Das Bakshi, P.H. Shipway, H.K.D.H. Bhadeshia, Three-body abrasive wear of fine pearlite, nanostructured bainite and martensite, Wear. 308 (2013) 46–53. https://doi.org/10.1016/j.wear.2013.09.008.

Accepted manuscript

[3] P.V. Moghaddam, J. Hardell, E. Vuorinen, B. Prakash, The role of retained austenite in dry rolling/sliding wear of nanostructured carbide-free bainitic steels, Wear. 428–429 (2019) 193–204. https://doi.org/10.1016/j.wear.2019.03.012.

[4] S. Das Bakshi, A. Leiro, B. Prakash, H.K.D.H. Bhadeshia, Dry rolling/sliding wear of nanostructured bainite, Wear. 316 (2014) 70–78. https://doi.org/10.1016/j.wear.2014.04.020.

[5] A. Leiro, E. Vuorinen, K.G. Sundin, B. Prakash, T. Sourmail, V. Smanio, F.G. Caballero, C. Garcia-Mateo, R. Elvira, Wear of nano-structured carbide-free bainitic steels under dry rolling-sliding conditions, Wear. 298–299 (2013) 42–47. https://doi.org/10.1016/j.wear.2012.11.064.

[6] L.C. Chang, The rolling/sliding wear performance of high silicon carbide-free bainitic steels, Wear. 258 (2005) 730–743. https://doi.org/10.1016/j.wear.2004.09.064.

[7] S.P. Neog, S. Das Bakshi, S. Das, Microstructural evolution of novel continuously cooled carbide free bainitic steel during sliding wear, Wear. (2020) 203359. https://doi.org/10.1016/j.wear.2020.203359.

[8] M. Shah, S. Das Bakshi, Three-body abrasive wear of carbide-free bainite, martensite and bainite-martensite structure of similar hardness, Wear. 402–403 (2018) 207–215. https://doi.org/10.1016/j.wear.2018.02.020.

[9] S.P. Neog, A.R. Kumar, S. Das Bakshi, S. Das, Understanding the complexities of dry sliding wear behaviour of steels, Mater. Sci. Technol. 37 (2021) 504–518. https://doi.org/10.1080/02670836.2021.1923136.

[10] A. García-Junceda, C. Capdevila, F.G. Caballero, C.G. de Andrés, Dependence of martensite start temperature on fine austenite grain size, Scr. Mater. 58 (2008) 134–137.

Accepted manuscript

https://doi.org/10.1016/j.scriptamat.2007.09.017.

[11] H.S. Yang, D.W. Suh, H.K.D.H. Bhadeshia, More Complete Theory for the Calculation of the Martensite–Start Temperature in Steels, ISIJ Int. 52 (2012) 164–166.

[12] A. Stormvinter, A. Borgenstam, J. Ågren, Thermodynamically based prediction of the martensite start temperature for commercial steels, Metall. Mater. Trans. A Phys. Metall. Mater. Sci. 43 (2012) 3870–3879. https://doi.org/10.1007/s11661-012-1171-z.

[13] J. Wang, S. Van der Zwaag, Stabilization mechanisms of retained austenite in transformation-induced plasticity steel, Metall. Mater. Trans. A. 32 (2001) 1527–1539. https://doi.org/10.1007/s11661-001-0240-5.

[14] X.C. Xiong, B. Chen, M.X. Huang, J.F. Wang, L. Wang, The effect of morphology on the stability of retained austenite in a quenched and partitioned steel, Scr. Mater. 68 (2013) 321–324. https://doi.org/10.1016/j.scriptamat.2012.11.003.

[15] S. Takaki, K. Fukunaga, J. Syarif, T. Tsuchiyama, Effect of grain refinement on thermal stability of metastable austenitic steel, Mater. Trans. 45 (2004) 2245–2251. https://doi.org/10.2320/matertrans.45.2245.

[16] K. Sugimoto, Ductility and strain-induced transformation in a high-strength transformation-induced plasticity-aided dual-phase steel, Metall. Trans. A. 23 (1992) 3085–3091. https://doi.org/10.1007/BF02646127.

[17] Y. Tomota, H. Tokuda, Y. Adachi, M. Wakita, N. Minakawa, A. Moriai, Y. Morii, Tensile behavior of TRIP-aided multi-phase steels studied by in situ neutron diffraction, Acta Mater. 52 (2004) 5737–5745. https://doi.org/10.1016/j.actamat.2004.08.016.

[18] K.S. Choi, W.N. Liu, X. Sun, M.A. Khaleel, Y. Ren, Y.D. Wang, Advanced

Accepted manuscript

micromechanical model for transformation-induced plasticity steels with application of in-situ high-energy X-ray diffraction method, Metall. Mater. Trans. A. 39A (2008) 3089–3096. https://doi.org/10.1007/s11661-008-9649-4.

[19] K. Sugimoto, A.K. Srivastava, Microstructure and Mechanical Properties of a TRIP-Aided Martensitic Steel, Metallogr. Microstruct. Anal. 4 (2015) 344–354. https://doi.org/10.1007/s13632-015-0221-5.

[20] C. Herrera, D. Ponge, D. Raabe, Design of a novel Mn-based 1 GPa duplex stainless TRIP steel with 60% ductility by a reduction of austenite stability, Acta Mater. 59 (2011) 4653–4664. https://doi.org/10.1016/j.actamat.2011.04.011.

[21] F. Lani, Q. Furnémont, T. Van Rompaey, F. Delannay, P.J. Jacques, T. Pardoen, Multiscale mechanics of TRIP-assisted multiphase steels: II. Micromechanical modelling, Acta Mater. 55 (2007) 3695–3705. https://doi.org/10.1016/j.actamat.2007.02.015.

[22] K.S. Choi, W.N. Liu, X. Sun, M.A. Khaleel, Microstructure-based constitutive modeling of TRIP steel: Prediction of ductility and failure modes under different loading conditions, Acta Mater. 57 (2009) 2592–2604. https://doi.org/10.1016/j.actamat.2009.02.020.

[23] R.G. Stringfellow, D.M. Parks, G.B. Olson, A constitutive model for transformation plasticity accompanying strain-induced martensitic transformations in metastable austenitic steels, Acta Metall. Mater. 40 (1992) 1703–1716. https://doi.org/10.1016/0956-7151(92)90114-T.

[24] R. Blondé, E. Jimenez-melero, L. Zhao, N. Schell, E. Brück, Mechanical stability of retained austenite in low-alloyed TRIP steel under shear loading, Mater. Sci. Eng. A.

Accepted manuscript

594 (2014) 125–134. https://doi.org/10.1016/j.msea.2013.11.001.

[25] I.Y. Pyshmintsev, M. De Meyer, B.C. De Cooman, R.A. Savray, V.P. Shveykin, M. Vermeulen, The Influence of the Stress State on the Plasticity of Transformation Induced Plasticity – Aided Steel, Metall. Mater. Trans. A. 33 (2002) 1659–1667.

[26] M.Y. Sherif, C.G. Mateo, T. Sourmail, H.K.D.H. Bhadeshia, Stability of retained austenite in TRIP-assisted steels, 20 (2004) 319–322. https://doi.org/10.1179/026708304225011180.

[27] W.R. Tyfour, J.H. Beynon, A. Kapoor, The steady state wear behaviour of pearlitic rail steel under dry rolling-sliding contact conditions, Wear. 180 (1995) 79–89. https://doi.org/10.1016/0043-1648(94)06533-0.

[28] D. Carlsson, D. Gren, Experimental Characterization of Pearlitic Rail Steel after Thermomechanical Strain- ing, Master's Thesis, Chalmers Univeristy Technol. (2019).

[29] J.H. Dautzenberg, J.H. Zaat, Quantitative determination of deformation by sliding wear, Wear. 23 (1973) 9–19. https://doi.org/10.1016/0043-1648(73)90036-7.

[30] W. Cai, P. Bellon, Subsurface microstructure evolution and deformation mechanism of Ag-Cu eutectic alloy after dry sliding wear, Wear. 303 (2013) 602–610. https://doi.org/10.1016/j.wear.2013.04.006.

[31] D.A. Hughes, N. Hansen, Graded nanostructures produced by sliding and exhibiting universal behavior, Phys. Rev. Lett. 87 (2001) 2–5. https://doi.org/10.1103/PhysRevLett.87.135503.

[32] S.I. Wright, M.M. Nowell, D.P. Field, M icroscopy M icroanalysis A Review of Strain Analysis Using Electron Backscatter Diffraction, 17 (2011) 316–329.

Accepted manuscript

Accepted for publication in Philosophical Magazine, DOI:
10.1080/14786435.2022.2139421

[33] M. Kamaya, A.J. Wilkinson, J.M. Titchmarsh, Quantification of plastic strain of stainless steel and nickel alloy by electron backscatter diffraction, Acta Mater. 54 (2006) 539–548. https://doi.org/10.1016/j.actamat.2005.08.046.

[34] S. Das, S. Kundu, A. Halder, A United States patent application publication: Pub. No.: US 2014/0102600 A1, 2014.

[35] S. Das, A. Haldar, Continuously cooled ultrafine bainitic steel with excellent strength-elongation combination, Metall. Mater. Trans. A. 45 (2014) 1844–1854. https://doi.org/10.1007/s11661-013-2173-1.

[36] S. Das, S. Sinha, A. Lodh, A.R. Chintha, M. Krugla, A. Haldar, Hot-rolled and continuously cooled bainitic steel with good strength–elongation combination, Mater. Sci. Technol. 33 (2017) 1026–1037. https://doi.org/10.1080/02670836.2016.1268663.

[37] S. Das, S. Kundu, A. Haldar, Development of continuously cooled high strength bainitic steel through microstructural engineering at Tata Steel, Mater. Sci. Forum. 702–703 (2012) 939–942. https://doi.org/10.4028/www.scientific.net/MSF.702-703.939.

[38] R. Rana, S. Chen, A. Haldar, S. Das, Mechanical properties of a bainitic steel producible by hot rolling, Arch. Metall. Mater. 62 (2017) 2331–2338. https://doi.org/10.1515/amm-2017-0342.

[39] ASTM International, Standard Test Method for Wear Testing with a Pin-on-Disk Apparatus G99-17, Annu. B. ASTM Stand. 05 (2017) 1–6. https://doi.org/10.1520/G0099-17.Copyright.

[40] D.V.S. Rao, K. Muraleedharan, C.J. Humphreys, TEM specimen preparation techniques, Microsc. Sci. Technol. Appl. Educ. (2010) 1232–1244.

Accepted manuscript

Accepted for publication in Philosophical Magazine, DOI:
10.1080/14786435.2022.2139421

[41] R. Alani, P.R. Swann, Preparation of high-quality ultrathin transmission electron microscopy specimens of a nanocrystalline metallic powder, Microsc. Res. Tech. 75(6) (2012) 711–719.

[42] D.J. Dyson, B. Holmes, Effect of alloying additions on the lattice parameter of austenite, J. Iron Steel Inst. 208 (1970) 469–474.

[43] TCFE7, TCS Steel and Fe-alloys Database TCFE7, (2012).

[44] S.P. Neog, S. Das Bakshi, S. Das, Effect of normal loading on microstructural evolution and sliding wear behaviour of novel continuously cooled carbide free bainitic steel, Tribol. Int. 157 (2021) 106846. https://doi.org/10.1016/j.triboint.2020.106846.

[45] A.M. Gola, M. Ghadamgahi, S.W. Ooi, Microstructure evolution of carbide-free bainitic steels under abrasive wear conditions, Wear. 376–377 (2017) 975–982. https://doi.org/10.1016/j.wear.2016.12.038.

[46] I. Hutchings, P. Shipway, Tribology, Friction and wear of engineering materials, Second edition, 2016.

[47] S. Shrivastava, C. Ghosh, J.J. Jonas, simple shear experiments A comparison of the von Mises and Hencky equivalent strains for use in simple shear experiments, (2012). https://doi.org/10.1080/14786435.2011.634848.

[48] S. Singh, Y. Guo, B. Winiarski, T.L. Burnett, P.J. Withers, M. De Graef, High resolution low kV EBSD of heavily deformed and nanocrystalline Aluminium by dictionary-based indexing, Sci. Rep. 8 (2018) 1–8. https://doi.org/10.1038/s41598-018-29315-8.

[49] S.I. Wright, M.M. Nowell, EBSD image quality mapping, Microsc. Microanal. 12 (2006) 72–84. https://doi.org/10.1017/S1431927606060090.

Accepted manuscript

Accepted for publication in Philosophical Magazine, DOI:
10.1080/14786435.2022.2139421

[50] K. Sugimoto, M. Tsunezawa, T. Hojo, S. Ikeda, Ductility of 0.1–0.6C–1.5Si–1.5Mn Ultra High-strength TRIP-aided Sheet Steels with Bainitic Ferrite Matrix, ISIJ Int. 44 (2004) 1608–1614.

[51] J.R. Patel, M. Cohen, Criterion for the action of applied stress in the martensitic transformation, Acta Metall. 1 (1953) 531–538.

[52] P.J. Jacques, J. Ladrière, F. Delannay, On the influence of interactions between phases on the mechanical stability of retained austenite in transformation-induced plasticity multiphase steels, Metall. Mater. Trans. A. 32 (2001) 2759–2768. https://doi.org/10.1007/s11661-001-1027-4.

Accepted manuscript



https://dspace.org/

Insights into the stability of retained austenite during wear

Neoga, Suruj Protim; Lodh, Arijit; Karmakar, Anish; Nair, Akhil G.; Dasgupta, Arup ...

2022-11-01
Taylor and Francis
https://doi.org/10.1080/14786435.2022.2139421
Neog SP, Lodh A, Karmakar A, et al., (2023) Insights into the stability of retained austenite during wear. Philosophical Magazine Part A: Materials Science, Volume 103, Issue 3, 2023, pp. 203-222

Downloaded from a DSpace repository. https://dspace.org/